Zipping into fusion

Zheng, T.

Chapter 5

Controlling the rate of coiled coil driven membrane fusion

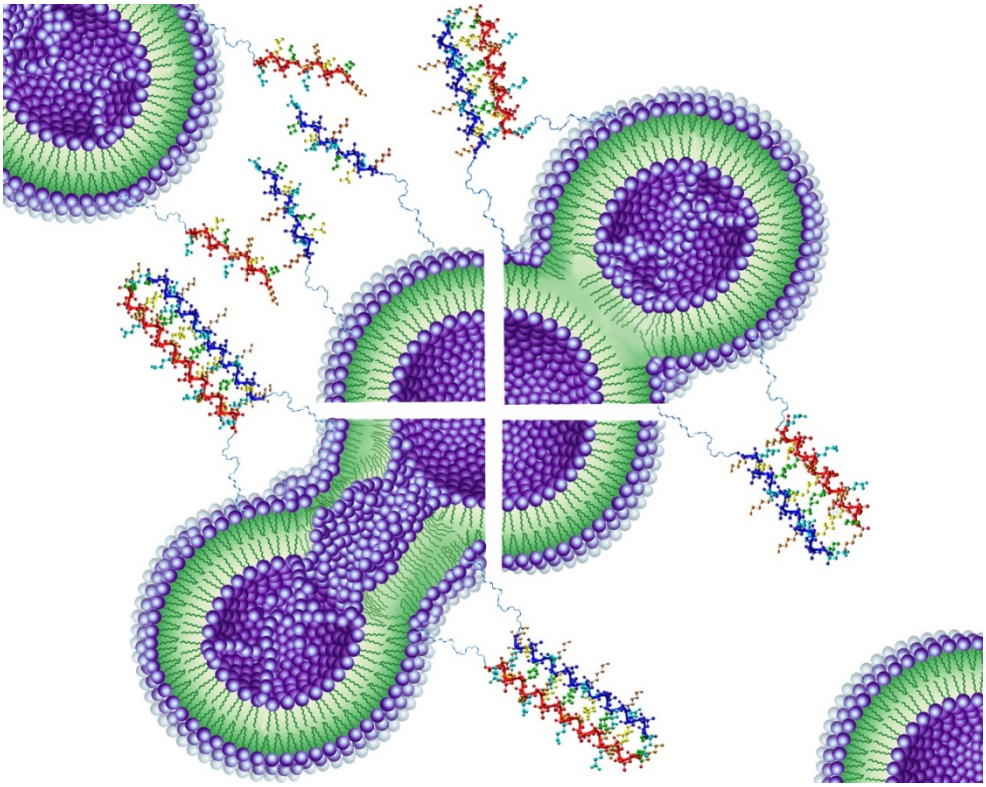

Zheng, T. T.; Voskuhl, J.; Versluis, F.; Zope, H. R.; Tomatsu, I.; Marsden, H. R.; Kros, A., Controlling the rate of coiled coil driven membrane fusion. Chemical Communications 2013, 49 (35), 3649-3651.

Abstract

Sets of complementary lipidated coiled-coil forming peptides inducing membrane fusion have been designed. The influence of the coiled-coil motif on the rate of liposome fusion was studied, by varying the number of heptad repeats. It was shown that an increased coiled-coil stability of complementary peptides translates into increased rates of membrane fusion of liposomes.

Introduction

The onset of supramolecular chemistry in recent decades has supplied scientists with a wealth of strategies to design functional materials.[1-7] The self-assembly of molecular components into well-defined supra structures is governed by non-covalent interactions. The careful orchestration of these weak molecular interactions allows for the rational design of supramolecular complexes with predictable and tunable properties.[8-14] Often, the inspiration for these assemblies comes from nature. Living systems display a staggering number of simultaneous orthogonal self-assembly processes. In particular, the well-defined secondary, tertiary and quaternary structures present in proteins have served as an invaluable motivation for research. For example, the specific recognition of DNA, RNA and carbohydrates, by proteins is based on the exact spatial placement of amino acid residues in the protein structure. With the rise of solid phase peptide chemistry it has become almost trivially easy to synthesize parts of proteins, i.e. peptides, with a well-defined amino acid structure and controllable self-assembly properties.[15-19] These peptides are therefore often able to mimic protein functions. An important area of research where this principle has been convincingly shown is membrane fusion. Membrane fusion is a vital process for the transport of molecules in all eukaryotic cells.[20-23] SNARE proteins are an important family of proteins which induce membrane fusion in vivo through the formation of a coiled coil complex and have been studied extensively.[24, 25] Recently, synthetic systems have been shown to promote membrane fusion based on specific interactions between a variety of fusogenic entities, such as peptides,[26-30] DNA[31-33] and other supramolecular recognition motifs.[34] Inspired by native SNARE proteins, our group has synthesized simplified SNAREs which are composed of a pair of coiled coil forming lipidated peptides (LPE and LPK). In our model system, molecular recognition between membrane bound peptides E and K leads to coiled coil formation, which drives fusion

between liposomes.[35] The synthetic lipopeptides consist of a hydrophobic tail (DOPE),a flexible linker (PEG_{12}) and coiled coil forming peptides E and K (Scheme 1). Peptides "E_3" $(EIAALEK)_3$ and "K_3" $(KIAALKE)_3$ consist of three heptad repeats, which form a heterodimeric coiled-coil motif upon binding.[36] The lipid tail ensures the efficient confinement of the peptide at the surface of the liposome. The advantage of our model system is that these peptide amphiphiles can be synthesized in a few days and chemical modifications can be easily introduced. Therefore, they can be tailored according to the needs of the particular application.

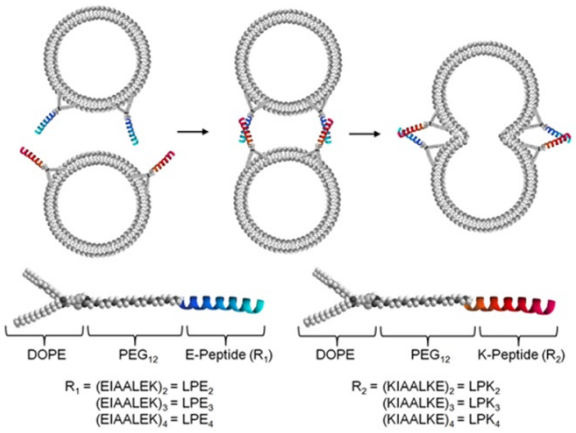

Scheme 1: Schematic illustration of liposome fusion mediated by lipopeptides, as well as an overview of the lipopetides used in this study. Liposomes are decorated with LPKx (red) or LPEx (blue) and upon mixing coiled-coil formation brings the opposite liposomes in close proximity, and ultimately leads to fusion.

Results and discussion

In this chapter, the relationship between the stability of the coiled-coil motif formed by the membrane bound peptides and the efficiency of liposome-liposome fusion process was investigated. Therefore three sets of lipidated coiled-coil forming peptides E_x-K_x composed of 2, 3 and 4 heptad repeat units were synthesized. It is envisaged that the peptide length could influence the efficiency of lipopeptide mediated fusion through the stability of the resulting coiled-coil complex. First, the stability of coiled-coils assembled from complementary acetylated peptides was evaluated using circular dichroism (CD) spectroscopy (Fig. 1). Coiled-coil unfolding as a function of temperature was followed by

measuring the ellipticity at 222 nm, which yields insights into the stability of all peptide pairs. First the symmetrical peptide pairs have been evaluated, i.e. peptide pairs with identical numbers of heptad repeats in each peptide. It was observed that the magnitude of the binding affinity was ordered as expected: K_4-E_4> K_3-E_3> K_2-E_2. The K_3-E_3 pair has a binding affinity of 11 kcal/mol at 25 ℃, whereas the values for K_4-E_4 and K_2-E_2 could not be determined as they are either too strong or too weak to be measured, respectively. Thus, increased coiled-coil stability is obtained upon increasing the peptide chain length, due to the increased number of non-covalent interactions between peptides E and K. Next, the ability to induce fusion between liposomes was studied for all symmetrical lipidated peptide pairs. First, a lipid mixing assay[37-39] was used to compare the extent of mixing of the membrane constituents of the liposomes (Fig. 2). In this assay, LPK_x decorated liposomes (with a hydrodynamic diameter of ~120 nm) contained the FRET pair DOPE-NBD (1,2-dioleoyl-sn-glycero-3-phosphoethanolamine-N-(7-nitro-2-1,3-benzoxadiazol-4-yl) and DOPE-LR (1,2-dioleoyl-sn-glycero-3-phosphatidylethanolamine-lissamine-rhodamine B), while the LPE_x decorated liposomes (~100 nm) did not contain any fluorescent label.

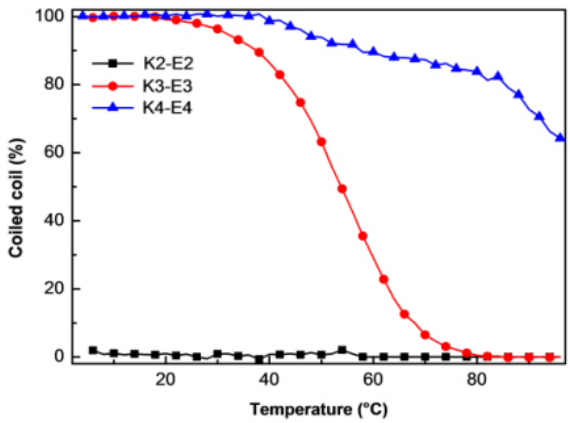

Figure 1: Thermal folding curve of E_x/K_x, as obtained from CD curves. [Total peptide] = 40 μM in PBS (pH=7.4, 50mM phosphate, 150mM NaCl).

Both sets of liposomes were stable in time and did not show any auto-fusion. However, upon mixing the two batches of liposomes, an increase in the NBD emission was observed due to the increased average distance between the NBD and LR dyes. This is indicative of

lipid mixing between the liposomes. Interestingly, a correlation between the stability of the coiled-coil motif and the extent of lipid mixing was observed. The largest fluorescence increase was found for liposomes decorated with LPK_4-LPE_4, followed by LPK_3-LPE_3 and finally LPK_2-LPE_2 (Fig. 2). The LPE_2/LPK_2 decorated liposomes show some degree of lipid mixing, even though the acetylated peptides E_2/K_2 are unable to form a coiled-coil complex. However, confinement of peptides at a lipid membrane interface induces α-helicity, even when these peptides adopt a random coil conformation in solution. This induced folding induces the complementary peptides to interact (see Table A2). Control experiments showed that lipid mixing only occurs when both complementary peptides are present and are able to form a coiled-coil motif, when one of the peptides is omitted, no lipid mixing occurs (Fig.2). Additional experiments were performed to investigate the effect of coiled-coil formation on the extent of lipid mixing as a function of temperature. Increasing the temperature from 25 ºC to 60 ºC led to strongly decreased lipid mixing for LPE_3-LPK_3 modified liposomes and no fusion at all was observed for LPE_2-LPK_2. In contrast, lipid mixing for LPE_4-LPK_4 decorated liposomes was hardly influenced (Fig. 2B). This observation is consistent with the CD measurements of the acetylated peptides, namely that E_3-K_3 show a decreased ability to assemble into coiled-coils upon raising the temperature to 60 °C, while E_4-K_4 remains predominantly in a coiled-coil formation. Several reports have shown that the fusion of liposomes can be halted at the hemifusion state, resulting in lipid mixing only.[21]

To test whether the trend in lipid mixing translated to full fusion events, a content mixing fluorescence assay was performed (Fig. 3). In this experiment, LPE-decorated liposomes were loaded with sulphorhodamine B at a self-quenching concentration (20 mM). Upon the addition of non-fluorescent LPK liposomes, content mixing results in a dilution of the dye, diminishing self-quenching and resulting in an increased fluorescent intensity. Consistent with the lipid mixing data, liposomes decorated with LPE_4 and LPK_4 showed the most efficient content mixing, followed by LPE_3 and LPK_3 and finally LPE_2 and LPK_2 (Fig 4). Again, this data correlates with the trend in the coiled-coil stability.

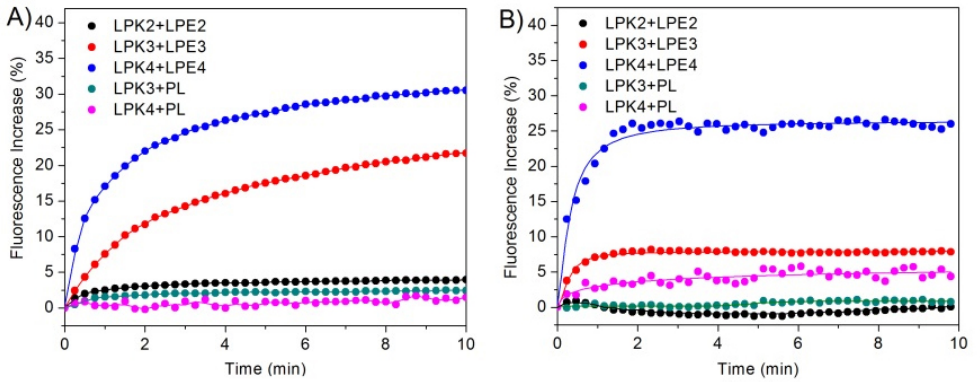

Figure 2. Fluorescence increase at A) 25 °C and B) 60 °C, due to lipid mixing between two batches of liposomes decorated with 1 mol% LPE_2-LPK_2, LPE_3-LPK_3, LPE_4-LPK_4. Two control experiments are shown; lipid mixing between $LPK_{3\ or\ 4}$-decorated liposome with plain liposomes (PL). [lipid] = 0.1 mM. LPK_x-decorated liposomes contained 0.5 mol% of DOPE-NBD and 0.5 mol% of DOPE-LR.

In addition, the evolution of particle sizes was measured upon mixing batches of LPE_x- and LPK_x-decorated liposomes using dynamic light scattering (DLS). Again, the strongest effect was observed for LPE_4 and LPK_4 modified liposomes, which is in good agreement with the content and lipid mixing assays. A summary of all fusion experiments, including content mixing (CM), lipid mixing (LM) and size increase (SI) measurements is given in table 1 and Figure 4. Next, the fusogenity of the various lipopeptide-decorated liposomes as a function of pH was investigated. This parameter strongly influences coiled-coil formation, since the peptides are designed to display opposite charges (Lys vs. Glu) at fixed sites of the assembly, controlling orientation and stability of the coiled-coil motif. The lipopeptide pairs LPE_3/LPK_3 and LPE_4/LPK_4 show significant lipid mixing throughout the studied pH range (pH 5-8, see Figure A16-19). Especially the peptide pair with four repeating heptads showed high lipid mixing values irrespective of pH , indicating that hydrophobic interactions are the driving force for coiled-coil formation, whereas the stabilization of the coiled-coil through opposite charges plays a minor role. These findings reveal that the E_4/K_4 coiled-coil binding motif can be used under a wide range of conditions (pH = 5-8, T = 25-60 °C). Finally, the properties of asymmetric peptide pairs have been evaluated, i.e. peptide pairs with a different number of heptad repeat units.

It was found for the acetylated peptides that both K_2/E_3 and K_3/E_2 showed no significant binding, which translated for the lipopeptides in negligible lipid mixing, content mixing and particle size increase (Table 1 and Figure 4). Large binding energies were found for

samples containing the acetylated pairs K_4/E_2 and K_2/E_4, although they were lower than for K_3/E_3.

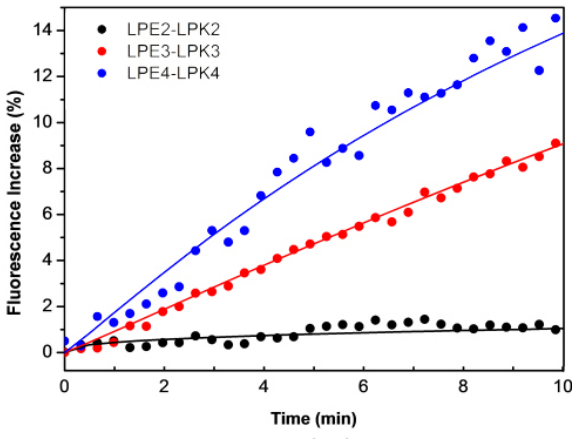

Figure 3: Content mixing assay; LPE_x decorated liposomes were loaded with 20 mM sulphorhodamine B and mixed with LPK_x liposomes. All spectra were obtained after mixing the liposomes. [total lipid] = 0.1 mM and 1% of lipopeptides LPE_4-LPK_4, LPE_3-LPK_3 or LPE_2-LPK_2, in HEPES buffer at pH = 7.2.

It is known that K_4 and E_4 form homocoils, complicating interpretation of binding energies. However, control lipid mixing experiments in which one lipopeptide from asymmetric pairs were omitted did not result in any significant lipid mixing (Fig. 2), indicating that asymmetric pairs do contribute to the observed binding energies.

Peptide	C-C[a]	BE[b]	T_m[c]	Lipopeptide	% CM[d]	% LM[e]	% SI[f]	R-LM[g]
Symmetric coiled-coil motifs								
K_2-E_2	-	-	-	LPK_2-LPE_2	1	4	0	2
K_3-E_3	+	11	58	LPK_3-LPE_3	9	21	148	8
K_4-E_4	+	n.d.	>96	LPK_4-LPE_4	14	31	176	17
Asymmetric coiled-coil motifs								
K_2-E_3	-	-	-	LPK_2-LPE_3	1	2	2	2
K_3-E_2	-	-	-	LPK_3-LPE_2	1	3	0	2
K_2-E_4	+	9	38	LPK_2-LPE_4	5	16	68	7
K_4-E_2	+	10	58	LPK_4-LPE_2	5	16	71	7
K_4-E_3	+	12	70	LPK_4-LPE_3	9	21	86	11
K_3-E_4	+	13	76	LPK_3-LPE_4	9	21	100	12

Table 1: Summary of coiled-coil formation studies of acetylated peptides and key data of liposome fusion studies using the lipidated peptide pairs LPE_x and LPK_x. [a]C-C = coiled coil; the + sign signifies the formation of a coiled-coil motif. [b] BE = binding energies in kcal/mol, [c] T_m = melting temperature in °C. n.d.= not determined. [d]CM = content mixing after 10 minutes, [e]LM = lipid mixing after 10 minutes, [f]SI = size increase of liposomes after 60 minutes, [g]R-LM=initial lipid mixing rate.

The strong tendency of the 4 heptad repeat peptides to form α-helices ensures the folding of the 2 heptad repeat peptides into α-helices upon binding. When confined to the surface of liposomes, these peptide pairs induced significant lipid and content mixing albeit to a lesser extent than E_3/K_4. Finally, samples containing the pairs K_4/E_3 and K_3/E_4 showed slightly higher binding energies than E_3/K_3 and yielded similar lipid and content mixing efficiencies. These results show that the stability of the coiled-coil pairs is reflected by the rate of fusion as determined by lipid and content mixing assays.

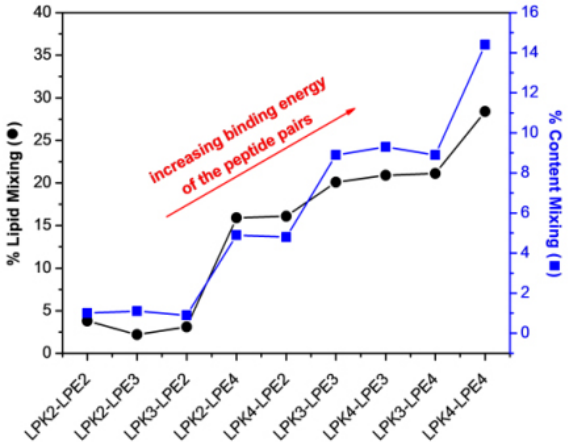

Figure 4: Correlation of lipid and content mixing to the coiled-coil lipidated peptide pairs with increasing stability.

Conclusion

In summary, the increased coiled-coil stability of complementary peptides translates into increased rates of membrane fusion of liposomes modified with the corresponding lipidated peptides, as observed by the different assays (content mixing, lipid mixing and size increase). Liposomes carrying lipidated peptides with 4 repeating units (i.e. E_4 and K_4) were found to be the most fusogenic, and can be used in a wide range of temperature and pH.

This lipopeptide induced fusion system can be applied beyond traditional membrane fusion, enabling the formation of complex supramolecular assemblies composed of nontraditional amphiphiles or to induce live cell fusion resulting in a direct drug delivery system.

Appendix

1. Materials and Methods

1.1 Materials

Fmoc-protected amino acids and Sieber Amide resin were purchased from Novabiochem. Fmoc-NH-PEG_{12}-COOH was purchased from IRIS Biotech. DOPC was purchased from Avanti Polar Lipids, DOPE was purchased from Phospholipid, and cholesterol was obtained from Fluka. DOPE-NBD and DOPE-LR were obtained from Avanti Polar Lipids, All other reagents and solvents were obtained at the highest purity available from Sigma-Aldrich or BioSolve Ltd. And used without further purification. Milli-Q water with a resistance of more than 18.2 MQ cm-1 was provided by a Millipore Milli-Q filtering system with filtration through a 22 um Millipak filter. Phosphate buffered saline, PBS: 5 mM KH_2PO4, 15mM K_2HPO_4, 150 mM NaCl, pH 7.4.

1.2 General Methods

RP-HPLC was performed with a Shimadzu HPLC system with two LC-8A pumps, and an SPD-10A VP UV-VIS detector, Sample elution was monitored by UV detection at 214nm and256nm. Sample elution was monitored by UV detection at 214nm and 256 nm. Samples were eluted with a linear gradient from A to B, A being ACN, and B 0.1% (V:V) TFA in H2O. Purification of the peptides and hybrids was performed on a C18 Vydac Column with a flow rated of 15ml/min. Sample purity was verified by LCMS. MALDI-TOF mass spectra were acquired using an Applied Biosystems Voyager System 6069 MALDI-TOF spectrometer with an ACH matrix. Samples were dissolved in 1:1 (v/v) 0.1% TFA in water:acetonitrile(TA), at concentrations of ~0.3mg/ml for K and E. Solutions for spots consisted of (V/V) 1:10 sample solution: 10 mg/ml ACH in TA. Phosphate buffered saline, PBS: 5 mM KH2PO4, 15 mM K2HPO4, 150 mM NaCl, pH 7.4.

2. Experimental details

2.1 Peptide Synthesis:

The peptides E_x and K_x were prepared using standard Fmoc-chemistry on a Syro-1 peptide synthesizer (Biotage). The peptides were synthesized on Sieber-Amide resin (0.62 mmol/g of NH_2). HCTU was used to activate the amino acids derivatives. The peptides were acetylated. Cleavage and de-protection was carried out using 95:2.5:2.5 (V/V)

TFA:H_2O:TIS for 1 hour. The cleavage mixture and three subsequent rinses of the resin with the TFA mixture were added drop-wise to cold diethyl ether. The white precipitate was compacted with centrifugation and the supernatant removed. This was repeated three times with the addition of fresh diethyl ether. The pellets were dried in air or under reduced pressure.

The crude products were purified by RP-HPLC. ACN used as mobile phase A, H_2O with 0.1% TFA as mobile phase B. Samples were eluted with a linear gradient from 90% to 10% B (V/V). After purification all compounds were lyophilized from water to give white material with typically a yield of 40% for all the peptides.

2.2 Lipopeptide synthesis:

The peptide components of LPE and LPK were prepared with standard solid-phase peptide synthesis protocols using Fmoc-chemistry on a Syro-1 automated peptide synthesizer (Biotage), with a PL-sieber Amide resin on a 0.25 mmol scale. The peptide coupling reagent was HCTU. The N-terminal Fmoc was removed with 20% (V/V) piperidine in NMP. After the peptide component was prepared, the resin was removed from the reaction vessel and Fmoc-NH-PEG_{12}-COOH was coupled to the immobilized peptides. The resin was swollen in NMP for 1 hour. 2.5 equivalents of Fmoc-NH-PEG_{12}-COOH and 2.5 equivalents of HCTU were dissolved in NMP(20ml) and mixed with 5 equivalents of DIPEA. After pre-activation for 1 minute the mixture was added to the peptide-resin and shaken for 20 hours. The uncoupled amines were capped with 0.05 M acetic anhydride, 0.125 M DIPEA in NMP. The N-terminal Fmoc was removed with 20% (V/V) piperidine in NMP. The resin was washed thoroughly with 10×10 ml DCM. Next, succinic anhydride was coupled to the immobilized peptide-PEG. The resin was swollen in NMP. 5 equivalents of succinic anhydride were dissolved in NMP (20mL) and mixed with 6 TEA. The mixture was added to the resin and shaken for 15 hours. The resin was washed thoroughly with 10×10mL NMP, and 10×10mL DCM. DOPE was coupled to the immobilized peptide-PEG_{12}-succinic acid in the same way, except that 3 equivalents of DOPE, 3 equivalents of HCTU, and 6 equivalents of DIPEA were used, and 1:1 (V/V) NMP: DCM was used to swell the resin and to couple the DOPE. After the peptide synthesis and after each subsequent coupling step the synthesis was tested by MALDI-TOF mass spectroscopy. Cleavage from the resin and deprotection was carried out by shaking 15 mg resin with 95: 2.5:2.5 (V/V) TFA:H_2O:TIS for one hour. The cleavage mixture and

three subsequent rinses of the resin with the TFA mixture were added drop-wise to cold diethyl ether. The white precipitate was compacted with centrifugation and the supernatant removed. This was repeated three times with the addition of fresh cold diethyl ether. The pellets were dried in air or under reduced pressure. Bulk cleavage of the compounds was performed in the same way except using Bulk cleavage of the compounds was performed in the same way except using 47.5: 47.5: 2.5: 2.5 (V/V) TFA: DCM: H_2O: TIS for one hour. The crude products were purified by RP-HPLC, the yield of LPE_2 and LPK_2 are 40%, LPK_4 30%, LPE_4 20%. For each compound the purity was estimated from RP-HPLC to be greater than 95%, with a mobile phase of 0.1% TFA ACN, and H_2O.

2.3 Electrospray ionization (ESI) mass spectrometry and HPLC

Lipopeptide	Molecular weight	HPLC purity
LPE_2	2952.8	> 95%
LPK_2	2950.9	> 95%
LPE_3	3706.2	> 95%
LPK_3	3703.4	> 95%
LPE_4	4461.6	> 95%
LPK_4	4458.3	> 95%

Table A1: Overview about calculated and found masses via MALDI-MS

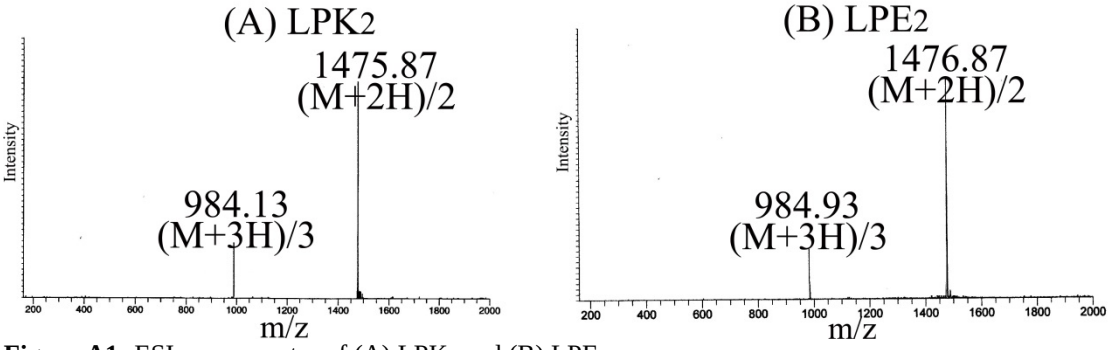

Figure.A1: ESI-mass spectra of (A) LPK_2 and (B) LPE_2.

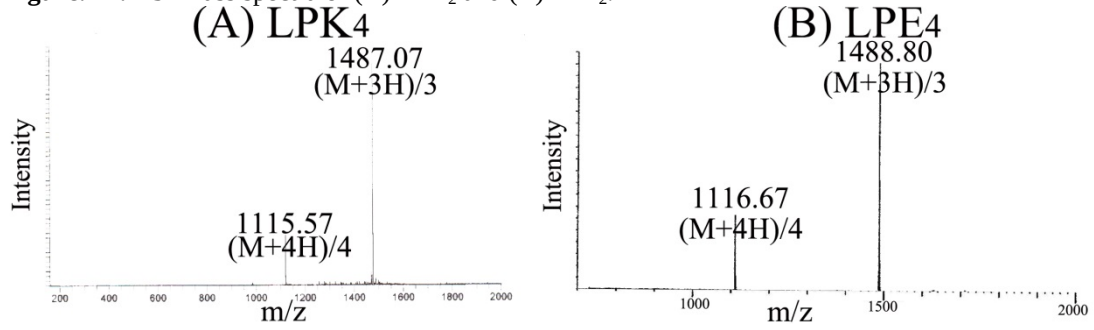

Figure.A2: ESI-mass spectra of (A) LPK_4 and (B) LPE_4

3. Liposomes

3.1 Liposome preparation:

1mM lipid stock solutions were made in chloroform with the composition DOPC/DOPE/CH 50:25:25 mol%. 1mM lipopeptide stock solutions were made in 1:1 (v/v) chloroform: methanol. Unless otherwise stated, liposome solutions are 1 mM in PBS. Three types of liposome solutions were prepared: plain liposomes, liposomes with 1 mol% LPE (99:1 (v/v) lipid stock solution: LPE stock solution), and liposomes with 1 mol% LPK (99:1 (v/v) lipid stock solution: LPK stock solution). To prepare small unilamellar vesicles the solvent was removed from the stock solution (2 mL) using a rotary evaporator to get a lipid film. Following this PBS (2 mL) was added to prepare a 1 mM liposome solution. The sample was vortexed for 1 minute and sonicated at 50 °C to form large unilamellar vesicles (it takes approximately 5 minutes for plain liposomes and 2 minutes for decorated liposomes respectively). The hydrodynamic diameter was approximately 100 nm as determined by DLS.

3.2 Content Mixing

Content mixing experiments were carried out as follows: A dried film containing DOPC/DOPE/CH 50:25:25 mol% and the corresponding E-Peptides (1 % of either LPE_2, LPE_3 or LPE_4) were hydrated and sonicated (5 min at 50°C) with a sulforhodamine B (20 mM) containing HEPES buffer solution (20 mM HEPES, 90 mM NaCl) at pH 7,2. The final lipid concentration was 1 mM. To get rid of non-encapsulated dye the liposomal solution was subjected to Sephadex (G50, Superfine) using HEPES (20 mM Hepes-Na, 90 mM NaCl) buffer as eluent. The fraction containing liposomes was collected and diluted to a final liposome concentration of 0.1 mM. 400 µL of the E-Peptide containing liposomes with encapsulated sulforhodamine B were added to a small volume disposable cuvette. The fluorescence signal of the Sulforhodamine (λ_{em} = 580 nm) was detected and another 400 µL of the corresponding K-Peptide containing liposomes (0.1 mM) in HEPES-buffer at pH = 7,2 were added and the increase of sulforhodamine B fluorescence, due to a relief of self-quenching, was detected. After a certain time 100 µL of 10% (v/v) solution of Triton X was added to lyse the liposomes and reach the maximum dilution. To calculate the percentage of fusion the following equation was used:

$$F\% = (F_{(t)} - F_{(0)} / (F_{(max)} - F_0) \times 100$$

where F(t) is the fluorescence at a certain time, $F_{(max)}$ is the fluorescence after lyses of the liposomes with Triton X and F(0) is the starting fluorescence after addition of the K-Peptide containing liposomes.

3.3 Lipid Mixing.

All spectra were obtained at room temperature using a quartz cuvette with a 1 cm path length. Liposomes consisting of DOPC/DOPE/CHOL/NBD-DOPE/RHD-DOPE (49.5/24.75/24.75/0.5/0.5 mol %) and 1 % of LPK_x where mixed with liposomes consisting of DOPC/DOPE/CHOL (59/25/25 mol %) and 1% of LPE_x. The NBD fluorescence was used to calculate the lipid mixing percentage with time. Fluorescence time series measurements were started immediately after mixing 750 µL of the fluorescent-labeled liposome suspension with 750uL of unlabeled liposome suspension in the cuvette. The NBD fluorescence intensity at 530 nm was monitored in a continuous fashion for 3000 seconds. After that the liposomes were lysed by the addition of 150 µL of 10 wt % Triton X-100 in PBS to obtain 100 % increments.

The values measured after lysis were multiplied by 1.82 to take into account the effect of Triton X-100 on the NBD fluorescence and dilution, which was obtained from a separate lysis experiment of a liposome solution that only contained DOPE-NBD. The percentage of fluorescence increase (%) is calculated as:

$$F(\%) = (F(t) - F0) / (F_{max} \times 1.82 - F_0) \times 100$$

where F(t) is the fluorescence intensity measured at time t, F_0 is the 0% fluorescence and F_{max} is the fluorescence intensity measured after addition of Triton X-100.

3.4 Initial fusion rate

The initial lipid mixing rate as characterization of the initial fusion rate and is calculated as:

$R=\Delta F/\Delta t$

ΔF stands for Fluoresce increase, Δt is time increase after 1:1 equimolar mix fluorescent label K liposome with non-fluorescent label E liposome. The increase in lipid mixing during the first minute of fusion is almost linear, therefore the increase in fluorescence in the first minute is used to calculate the rate of fusion.

4. Additional measurements

4.1 Circular Dichroism Spectroscopy

4.1.1 Peptide conformation and binding energy assay:

CD spectra were obtained using a Jasco J-815 spectropolarimeter equipped with a peltier controlled thermostatic cell (Fig. A3,4). The ellipticity is given as mean residue molar ellipticity, $[\theta](10^3 deg cm^2 dmol^{-1})$, calculated by Eqn. (1),

$$[\theta]= (\theta_{obs} \times MRW)/(10 \times lc) \quad (1)$$

Where θ_{obs} is the ellipticity in millidegrees, MRW is the mean residue molecular weight, l is the path length of the cuvette in cm and c is the peptide concentration in mg/mL.

A 1.0mm quartz cuvette and 200 µM concentration of peptide in pH=7.4 PBS were used for detection of the peptide secondary structure. Spectra were recorded from 260nm to 200nm at 25°C. Data was collected at 0.5nm intervals with a 1nm bandwidth and 1s readings. Each spectrum was the average of 5 scans. For analysis each spectrum had the appropriate background spectrum subtracted.

Temperature dependent CD spectra (Fig. A3,4) for calculation of the peptide binding energy were obtained using an external temperature sensor immersed in the sample. The temperature was controlled with the internal sensor and measured with the external sensor. A 10 mm quartz cuvette was used, and the solutions were stirred at 900 rpm. Spectra were recorded from 260 nm to 200 nm, with data collected at 0.5 nm intervals with a 1 nm bandwidth and 1 s readings. Each spectrum was one scan. The temperature range was 6 °C to 96 °C with a temperature gradient of 2.0°C/minute and a 60 s delay after reaching the set temperature. The solutions took 5 minutes to return to 6 °C. The spectrum of PBS at 6 °C (average of 5 scans) was subtracted from each spectrum.

The data was analyzed using a two-state unfolding model to determine the fraction folded using Eqn. (2),

$$F_f=([\theta]-[\theta]_U)/([\theta]_F-[\theta]_U) \quad (2)$$

Where $[\theta]$ is the observed molar ellipticity, $[\theta]_U$ is the ellipticity of the denatured state, as determined from the plateau of the ellipticity vs. temperature curve, and $[\theta]_F$ is the ellipticity of the folded state at that temperature as determined from a linear fit of the initial stages of the ellipticity vs. temperature curve.

The fraction unfolded, FU, was calculated by Eqn. (3),

$$F_U=1-F_f \quad (3)$$

The dimer dissociation constant in the transition zone was calculated using Eqn. (4),

$K_U=2P_tF_U^2/F_f$ (4)

Pt is the total peptide concentration. By taking the derivative of the $\ln(K_U)$ vs. Temperature and using this in the van't Hoff equation, Eqn. (5), the change in enthalpy associated with unfolding with temperature can be plotted:

$d\ln(K_U)/dT=\Delta H_U/RT^2$ (5)

The gradient of this plot ΔCp, is the difference in heat capacity between the folded and unfolded forms, and can be used in the Gibbs-Helmholtz equation adapted to monomer-dimer equilibrium, Eqn. (6), to obtain the Gibbs free energy of unfolding as a function of temperature

$\Delta G_U=\Delta H_m(1-T/T_m)+\Delta C_p[T-T_m-T\ln(T/T_m)]-RT\ln[P$ (6)

T_m and H_m, the temperature and enthalpy at the midpoint of the transition, is determined by the maximum of derivative of the ellipticity vs. temperature graph.

All binding energy calculations were based on the assumption that the peptide pairs form a 1:1 heterodimer complex (1:1 complex of E_x and K_x).

With the formula above, the binding energy of E/K complex from the graphs below has been calculated (Fig. A3,4):

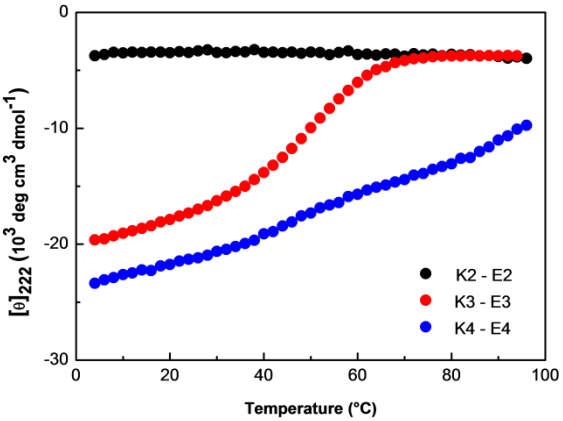

Figure.A3: Temperature dependent CD spectra monitored molar ellipticity changing at 222nm. K_m/E_n pairs in 20mM phosphate, 150mM NaCl, pH 7.4, [Total peptide] = 40 µM.

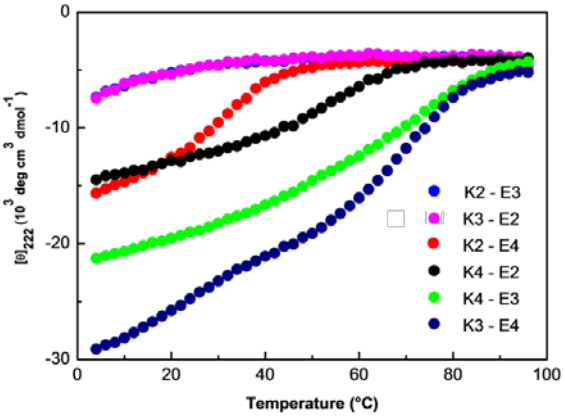

Figure A4: Temperature dependent CD spectra monitored molar ellipticity changing on wavelength 222nm. K_m/E_n pairs in 20mM phosphate, 150mM NaCl, pH 7.4, [Total peptide] = 40µM.

Figure A5 and A6 show the temperature dependent CD-spectra for E_3-K_3 and with E_4-K_4. With increasing temperature the E3-K3 coiled coil dissociates, but the E_4-K_4 coiled coil still exists even when the temperature reaches 96 °C.

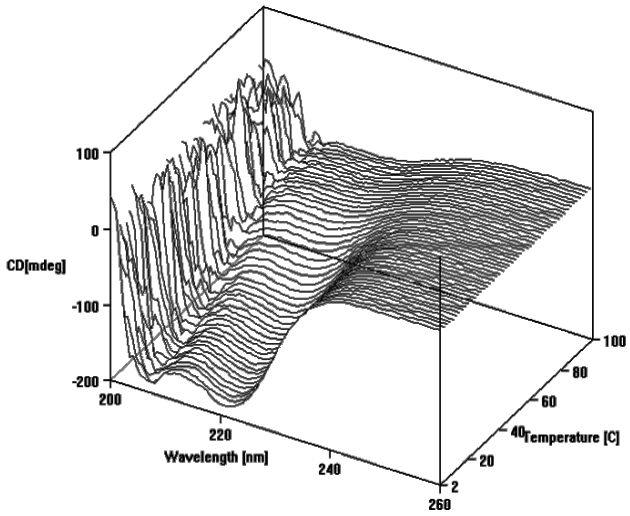

Figure.A5: 3D spectrum of the E_3/K_3 coiled-coil complex ellipticity upon increasing the temperature from 2-96°C.

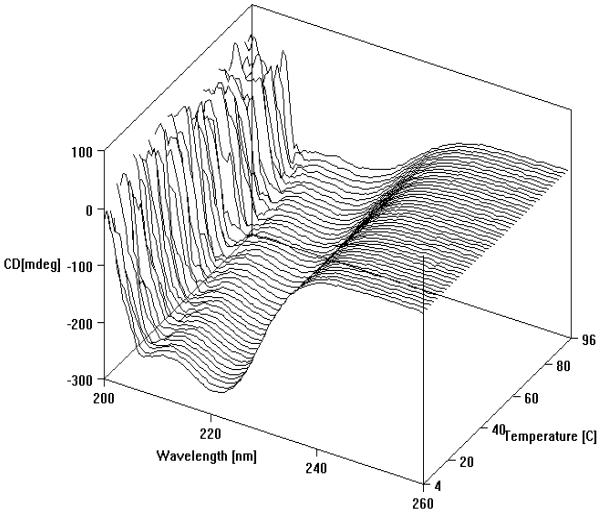

Figure A6: 3D spectrum of E4/K4 coiled coil complex ellipticity following by the temperature increasing from 2-96°C.[36.]

4.1.2 Determination of the percentage α-helix and the confirmation coiled-coils

The percentage α-helicity is the ratio of the observed $[\theta]_{222}$ to the predicted $[\theta]_{222}$ for an α-helical peptide of n residues ×100. The predicted $[\theta]_{222}$ = -40000×(1-4.6/n).[40] Peptide interactions were further confirmed by TFE-CD measurements. TFE is known to enhance intramolecular α-helicity but decrease intermolecular interactions.[41]. Equimolar E and K mixture has been measured first in PBS, then TFE: PBS 1:1 (v/v). If there is a significant decrease in the in the $[\theta]_{222}/[\theta]_{208}$ ratio from PBS to 50% TFE in PBS, one can assume, that there is a destruction of the coiled-coil binding motif. Here total peptide concentration is 1 mg /mL in 50 mM phosphate, 150 mM NaCl, pH 7.4, 25°C.

Peptide	θ_{222}		%α-helix		$\theta_{222}/\theta_{208}$		Coiled-coil
	PBS	50%TFE	PBS	50%TF	PBS	50%TFE	
E2	-2490	-17718	9	66	0.50	0.73	-
K2	-1876	-14142	7	53	0.32	0.73	-
E2+K2	-3561	-17786	13	66	0.37	0.73	-
E3	-5819	-22465	19	72	0.59	0.84	-
K3	-6638	-23139	21	74	0.73	0.84	-
E3+K3	-24705	-23277	79	75	1.10	0.90	+
E4	-22173	-23176	66	69	1.43	0.86	+
K4	-24714	-25812	74	77	1.25	0.86	+
E4+K4	-31066	-31341	93	94	1.11	0.90	+

Table A1.: Concentrations of the peptides: 1mg/ml, Buffer 50mM phosphate, 150mM NaCl, pH 7.4, 25°C.

4.1.3 Comparison of secondary structure of E_2, K_2 and liposomes modified with LPE_2 and LPK_2.

Peptide	% α-helicity		Peptide	% α-helicity
Ac-E2	9		LPE2	20
Ac-K2	7		LPK2	19
Ac-E2+Ac-K2	13		LPE2+LPK2	40

Table A2. Comparision of acetylated E2,K2, E2+K2 percentage of alpha-helix changed from uniform disperse in buffer with fixed on surface of liposome. Acetylated peptide were measured in pH=7.4 PBS buffer (PBS buffer as baseline), 25℃. LPE2, LPK2 and LPE2+LPK2 were decorated on surface of liposome to make them water-soluble (plain liposome in same buffer as baseline). All the acetylated peptide were measured in 1mg/ml concentration, 1 mm cuvette was used, 4 scans for each peptide, while all the lipopeptide were decorated 1% on liposome surface which compose of 0.5mM lipid in pH=7.4 PBS in 5mm cuvette on 25℃,6 scans for each lipopeptide.

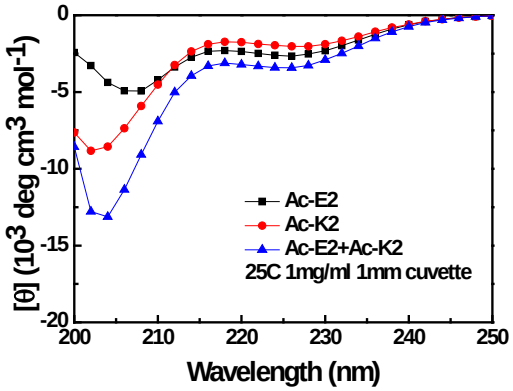

Figure A7: CD spectroscopic data of acetylated E2, K2 and E2-K2 complex. 1mg/ml peptides in pH=7.4 PBS (50mM phosphate, 150mM NaCl) were measured with 1mm cuvette on 25℃.

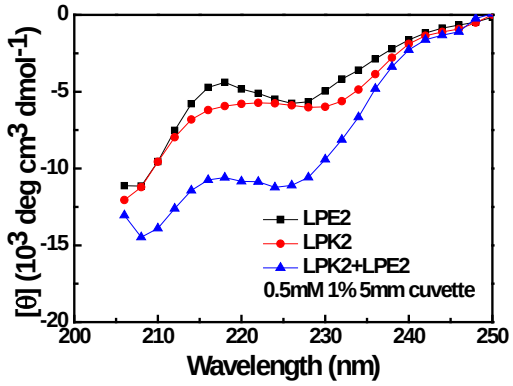

Figure A8: CD spectroscopic data of LPE2, LPK2, LPE2+LPK2 complex. All lipopeptide were decorated on surface of liposome, to make them water soluble, meanwhile use plain liposome as baseline during all the lipopeptide-liposome measurements. All the samples content 0.5mM lipid and 1% lipopeptide, and measured by 5mm cuvette was used on 25℃.

4.2 Lipid Mixing (Cross combinations)

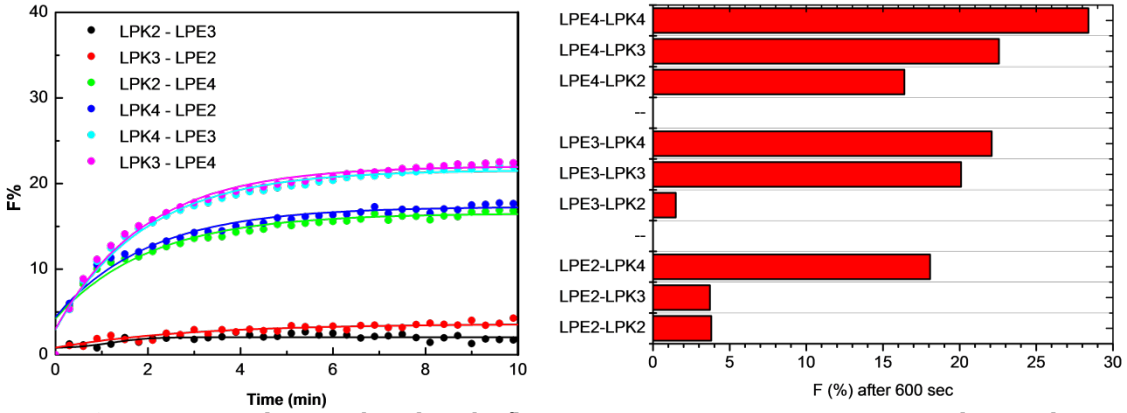

Figure A9: Lipid mixing based on the fluorescence increase upon mixing LPK_x decorated fluorescent liposomes and LPE_x decorated liposomes.

4.3 Content mixing (cross combinations)

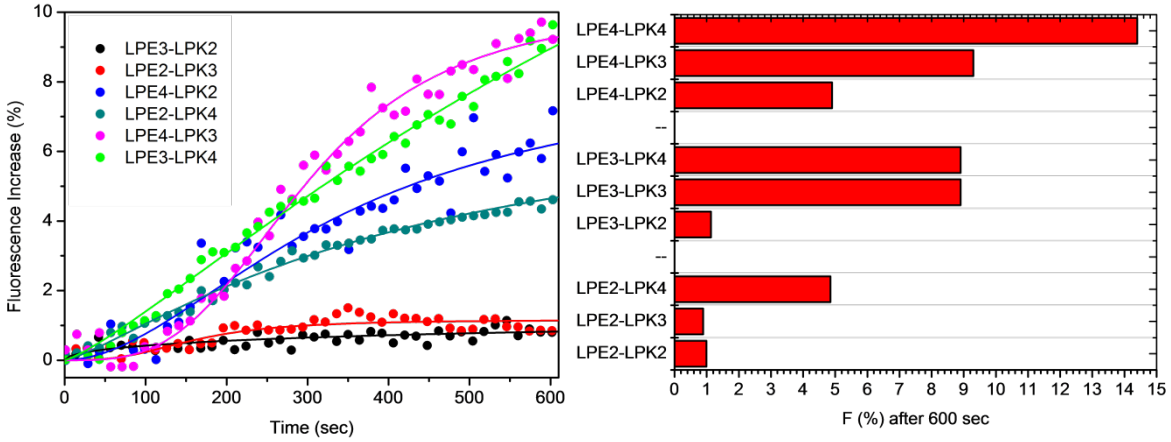

Figure A10: Lipid mixing based on the fluorescence increase upon mixing LPK_x decorated liposomes and LPE_x decorated liposomes with encapsulated sulphorhodamine (20 mM).

4.4 Dynamic light scattering (cross combinations)

Hydrodynamic diameters were estimated at 25 °C by dynamic light scattering using a Malvern Zetasizer Nano ZS ZEN3500 equipped with a peltier-controlled thermostatic cell holder. The laser wavelength was 633 nm and the scattering angle was 173°. For individual liposome batches the samples were allowed to equilibrate for 2 minutes. For DLS time series the solutions were mixed in the cuvette for 30 second. Measurements were started immediately after mixing without 2 minutes of

sample equilibration, and continued for 1h:

Size increase % = $100*(S_{1h}-S_0)/S_0$

(S_{1h}: Zeta average diameter after 1 hour mixing, S_0: Zeta average diameter immediately after mixing).

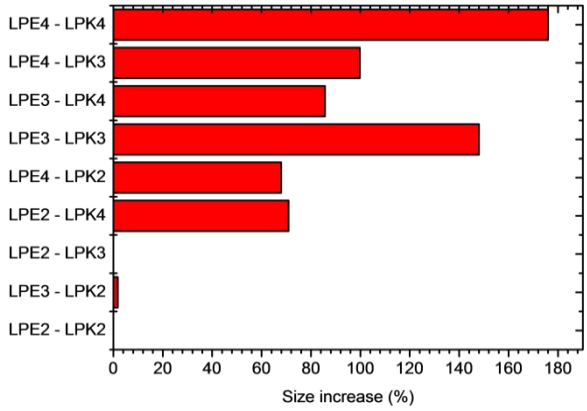

Figure A11: Size increase in percentage of all cross combination.

4.5 Comparison of different conditions

4.5.1 Rate of fusion as a function of temperature:

The same method that mentioned in main text for the lipid mixing has been applied, except, that a controllable water bath was used to determine the lipid mixing at different temperature.

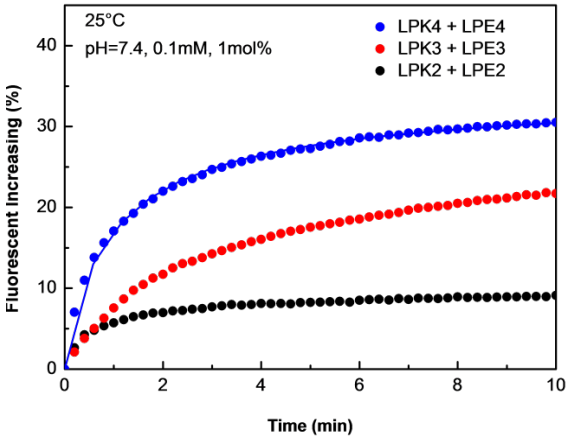

Figure A12 : Lipid mixing at, pH=7.4.

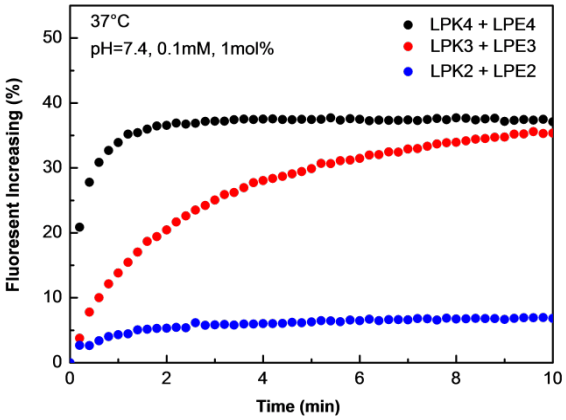

Figure A13 Lipid mixing at 37°C, pH=7.4.

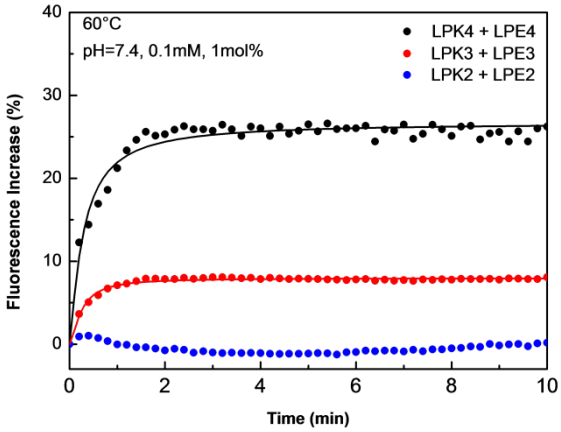

Figure A14: Lipid mixing at 60 °C, pH=7.4.

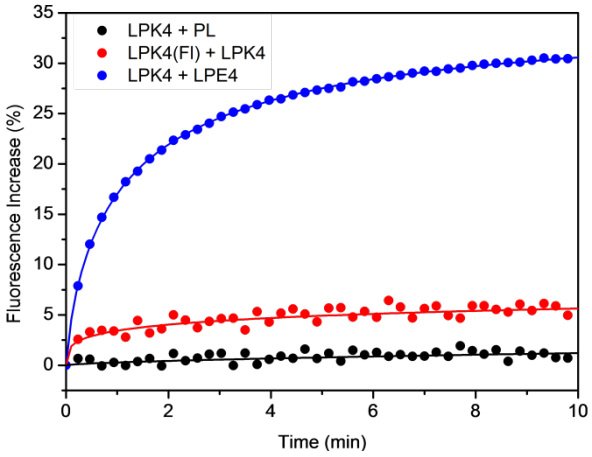

Figure A15: Lipid Mixing at 25°C, Control experiments, pH = 7,4.

4.5.2 Rate of fusion as a function of pH:

The same lipid mixing method as mentioned before has been performed, except, that the pH was varied.

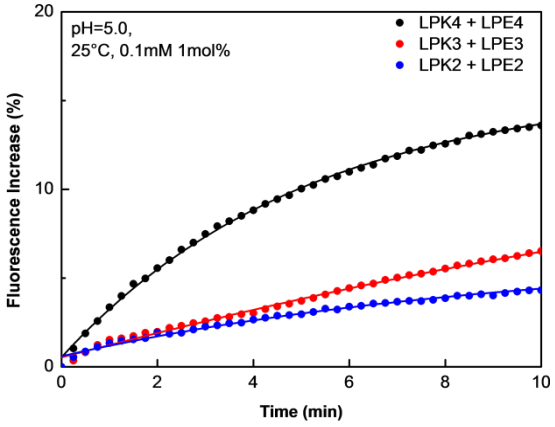

Figure A16: Liposome fusion at 25°C, pH=5.0.

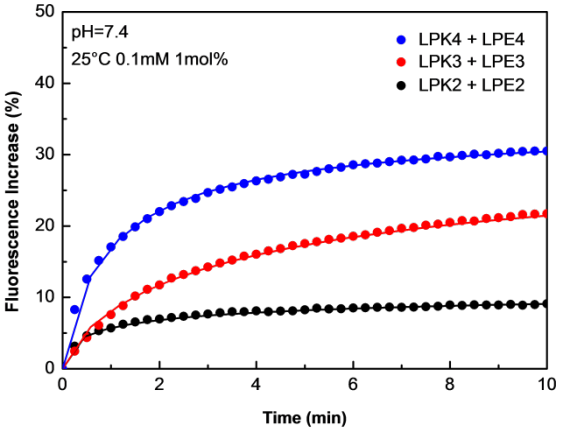

Figure A17: Liposome fusion at 25 °C pH=7.4.

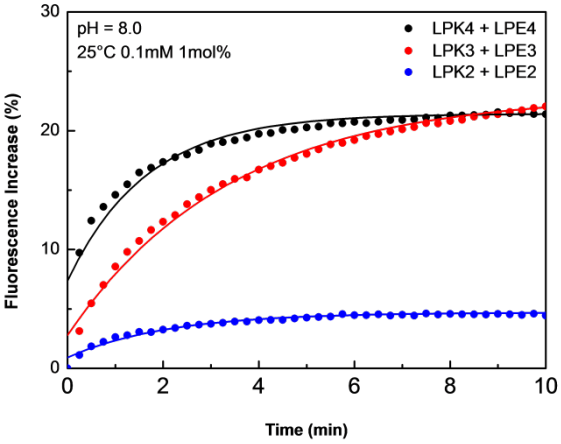

Figure A18: Liposome fusion at 25°C, pH=8.0.

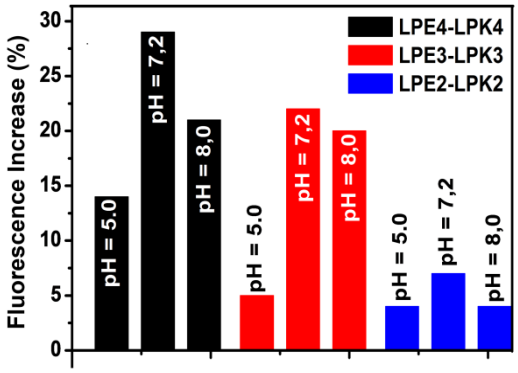

Figure A19: Comparison of lipid mixing of LPE_x-LPK_x modified liposomes as a function of pH.

Reference

1. J. M. Lehn, *Angewandte Chemie-International Edition in English*, 1990, **29**, 1304-1319.
2. J. H. van Esch and B. L. Feringa, *Angewandte Chemie-International Edition*, 2000, **39**, 2263-2266.
3. Z. Liu, X. Sun, N. Nakayama-Ratchford and H. Dai, *Acs Nano*, 2007, **1**, 50-56.
4. T. Kato, N. Mizoshita and K. Kishimoto, *Angewandte Chemie-International Edition*, 2006, **45**, 38-68.
5. J. Elemans, A. E. Rowan and R. J. M. Nolte, *Journal of Materials Chemistry*, 2003, **13**, 2661-2670.
6. A. R. Hirst, B. Escuder, J. F. Miravet and D. K. Smith, *Angewandte Chemie-International Edition*, 2008, **47**, 8002-8018.
7. L. He, Y. Jiang, C. Tu, G. Li, B. Zhu, C. Jin, Q. Zhu, D. Yan and X. Zhu, *Chemical Communications*, 2010, **46**, 7569-7571.
8. A. R. Hirst and D. K. Smith, *Chemistry-a European Journal*, 2005, **11**, 5496-5508.
9. J. Voskuhl and B. J. Ravoo, *Chemical Society Reviews*, 2009, **38**, 495-505.
10. J. W. Steed, *Chemical Society Reviews*, 2010, **39**, 3686-3699.
11. S. Chiruvolu, S. Walker, J. Israelachvili, F. J. Schmitt, D. Leckband and J. A. Zasadzinski, *Science*, 1994, **264**, 1753-1756.
12. C. Schmuck and W. Wienand, *Angewandte Chemie-International Edition*, 2001, **40**, 4363-+.
13. F. Versluis, J. Voskuhl, M. C. A. Stuart, J. B. Bultema, S. Kehr, B. J. Ravoo and A. Kros, *Soft Matter*, 2012, **8**, 8770-8777.
14. S. Trier, J. R. Henriksen and T. L. Andresen, *Soft Matter*, 2011, **7**, 9027-9034.
15. R. V. Ulijn and A. M. Smith, *Chemical Society Reviews*, 2008, **37**, 664-675.
16. C. Tomasini and N. Castellucci, *Chemical Society Reviews*, 2013, **42**, 156-172.
17. Y. C. Yu, P. Berndt, M. Tirrell and G. B. Fields, *Journal of the American Chemical Society*, 1996, **118**, 12515-12520.
18. F. Versluis, H. R. Marsden and A. Kros, *Chemical Society Reviews*, 2010, **39**, 3434-3444.
19. D. N. Woolfson and Z. N. Mahmoud, *Chemical Society Reviews*, 2010, **39**, 3464-3479.
20. R. Jahn, T. Lang and T. C. Sudhof, *Cell*, 2003, **112**, 519-533.
21. H. R. Marsden, I. Tomatsu and A. Kros, *Chemical Society Reviews*, 2011, **40**, 1572-1585.
22. J. M. White, *Science*, 1992, **258**, 917-924.
23. B. R. Lentz, *European Biophysics Journal with Biophysics Letters*, 2007, **36**, 315-326.
24. T. Weber, B. V. Zemelman, J. A. McNew, B. Westermann, M. Gmachl, F. Parlati, T. H. Sollner and J. E. Rothman, *Cell*, 1998, **92**, 759-772.
25. R. B. Sutton, D. Fasshauer, R. Jahn and A. T. Brunger, *Nature*, 1998, **395**, 347-353.

26. H. R. Marsden, N. A. Elbers, P. H. H. Bomans, N. A. J. M. Sommerdijk and A. Kros, *Angewandte Chemie-International Edition*, 2009, **48**, 2330-2333.
27. H. R. Marsden and A. Kros, *Angewandte Chemie-International Edition*, 2010, **49**, 2988-3005.
28. A. Kashiwada, M. Tsuboi and K. Matsuda, *Chemical Communications*, 2009, 695-697.
29. A. Kashiwada, M. Tsuboi and K. Matsuda, *Langmuir*, 2011, **27**, 1403-1408.
30. A. Kashiwada, M. Tsuboi, N. Takamura, E. Brandenburg, K. Matsuda and B. Koksch, *Chemistry-a European Journal*, 2011, **17**, 6179-6186.
31. Y.-H. M. Chan, B. van Lengerich and S. G. Boxer, *Proceedings of the National Academy of Sciences of the United States of America*, 2009, **106**, 979-984.
32. G. Stengel, R. Zahn and F. Hook, *Journal of the American Chemical Society*, 2007, **129**, 9584-+.
33. G. Stengel, L. Simonsson, R. A. Campbell and F. Hook, *Journal of Physical Chemistry B*, 2008, **112**, 8264-8274.
34. Y. Gong, M. Ma, Y. Luo and D. Bong, *Journal of the American Chemical Society*, 2008, **130**, 6196-6205.
35. I. Tomatsu, H. R. Marsden, M. Rabe, F. Versluis, T. Zheng, H. Zope and A. Kros, *Journal of Materials Chemistry*, 2011, **21**, 18927-18933.
36. J. R. Litowski and R. S. Hodges, *Journal of Biological Chemistry*, 2002, **277**, 37272-37279.
37. N. Duzgunes, T. M. Allen, J. Fedor and D. Papahadjopoulos, *Biochemistry*, 1987, **26**, 8435-8442.
38. D. Hoekstra and N. Duzgunes, *Methods in Enzymology*, 1993, **220**, 15-32.
39. D. K. Struck, D. Hoekstra and R. E. Pagano, *Biochemistry*, 1981, **20**, 4093-4099.
40. Y. H. Chen, J. T. Yang and K. H. Chau, *Biochemistry*, 1974, **13**, 3350-3359.
41. S. Y. M. Lau, A. K. Taneja and R. S. Hodges, *Journal of Biological Chemistry*, 1984, **259**, 3253-3261.